**Atmospheric
Chemistry
and Physics**

Eddy covariance flux measurements of biogenic VOCs during ECHO 2003 using proton transfer reaction mass spectrometry

C. Spirig[1], A. Neftel[1], C. Ammann[1], J. Dommen[2], W. Grabmer[3], A. Thielmann[4], A. Schaub[5], J. Beauchamp[3], A. Wisthaler[3], and A. Hansel[3]

[1]Agroscope, Swiss Federal Research Station for Agroecology and Agriculture, Reckenholzstr. 191, 8046 Zürich, Switzerland
[2]Laboratory of Atmospheric Chemistry, Paul Scherrer Institut, Villigen, Switzerland
[3]Institute of Ion Physics, University of Innsbruck, Austria
[4]Max Planck Institute for Chemistry, Mainz, Germany
[5]Research Centre Jülich, Germany

Abstract. Within the framework of the AFO 2000 project ECHO, two PTR-MS instruments were operated in combination with sonic anemometers to determine biogenic VOC fluxes from a mixed deciduous forest site in North-Western Germany. The measurement site was characterised by a forest of inhomogeneous composition, complex canopy structure, limited extension in certain wind directions and frequent calm wind conditions during night time. The eddy covariance (EC) technique was applied since it represents the most direct flux measurement approach on the canopy scale and is, therefore, least susceptible to these non-ideal conditions. A specific flux calculation method was used to account for the sequential multi-component PTR-MS measurements and allowing an individual delay time adjustment as well as a rigorous quality control based on cospectral analysis. The validated flux results are consistent with light and temperature dependent emissions of isoprene and monoterpenes from this forest, with average daytime emissions of 0.94 and $0.3\,\mu g\ m^{-2}\,s^{-1}$, respectively. Emissions of methanol reached on average $0.087\,\mu g\ m^{-2}\,s^{-1}$ during daytime, but fluxes were too small to be detected during night time. Upward fluxes of the isoprene oxidation products methyl vinyl ketone (MVK) and methacrolein (MACR) were also found, being two orders of magnitude lower than those of isoprene. Calculations with an analytical footprint model indicate that the observed isoprene fluxes correlate with the fraction of oaks within the footprints of the flux measurement.

1 Introduction

Volatile organic compounds (VOCs) emitted by terrestrial vegetation represent a major source of reactive carbon to the atmosphere on a global scale. Locally, biogenic VOCs (BVOCs) may contribute significantly to the formation of ozone and particulate matter. In the perspective of carbon budgets on the ecosystem level, the amount of carbon released as BVOCs can reach a significant fraction of the net carbon uptake (net ecosystem productivity, NEP) (Guenther, 2002; Kesselmeier et al., 2002). When assessing the impacts of these natural sources of VOCs on air quality and climate, it is not only important to know these emissions, but also their fate once they are released. These were the major goals of ECHO (Emission and CHemical transformation of biogenic volatile Organic compounds), a project of the German atmospheric research program Atmosphärenforschung (AFO) 2000. ECHO included various laboratory studies and two major field campaigns in the summers of 2002 and 2003, designed to investigate both emissions and chemical transformation of BVOCs within and above a forest canopy.

Key information in this context are the different BVOC fluxes out of the vegetation canopy. Measurements and estimates of this quantity have been reported for a variety of ecosystems throughout the last years. They stem from enclosure studies (e.g. Lamb et al., 1985), gradient techniques (Guenther et al., 1996) and more recently from the eddy covariance (EC) method or derivatives of it (relaxed eddy accumulation, REA (Baker et al., 1999) and disjunct eddy covariance, DEC (Karl et al., 2002; Rinne et al., 2001)). The EC method directly determines the vertical flux of a trace component by measuring the covariance between fluctuations in vertical wind velocity and the mixing ratios of
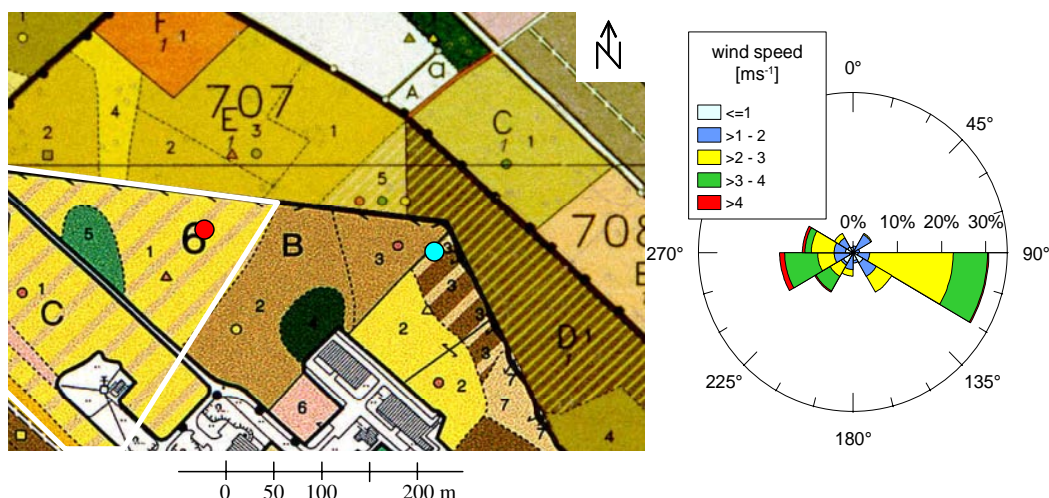
Fig. 1. Map of the ECHO site with the locations of the west (red circle) and main tower (blue circle). The colours represent forest areas with different dominating tree species, oak dominated forests are yellow, brown areas indicate beech sections. The wind rose indicates the distribution of daytime winds during the measurement period (13–25 July 2003).

the trace components. The key analytical issue for using the direct EC approach to simultaneously measure fluxes of several compounds is the availability of an appropriate sensor: It must be capable to measure these components fast enough and with high sensitivity. Several years ago, the company Ionicon Analytik GmbH (Innsbruck, Austria) made the technique of Proton-Transfer-Reaction Mass-Spectrometry (PTR-MS) commercially available. PTR-MS can measure many of the relevant BVOCs at their typical ambient concentrations (Lindinger et al., 1998). Karl et al. (2001) have demonstrated that a redesigned model of the original Ionicon instrument is able to perform direct EC measurements of a wider suite of compounds.

We applied two PTR-MS instruments in combination with the EC technique to directly measure the vertical fluxes of several BVOCs at the ECHO field site, a mixed deciduous forest on the area of the Research Centre Jülich in North-Western Germany. While this field site is ideal for deploying bulky instruments for measuring chemical species usually limited to investigations in the laboratory, it is a challenging place for doing flux measurements. The forest is non-homogenous both in species composition and canopy structure, and its extension in certain wind directions is less than 100 meters. Under these circumstances, the determination of fluxes by the EC technique requires careful evaluation and quality control.

2 Experimental

2.1 The ECHO site and instrumental setup

The 2003 intensive investigation period of ECHO took place at the Research Centre Jülich, west of Cologne, Germany.

The research site consists of a mixed deciduous forest with beech, birch and oak as dominating tree species. Figure 1 shows an overview of the forest with the location of the two towers (in the following referred to as "main tower" and "west tower") that served as platforms for the measurements discussed in this paper. The west tower is surrounded by a 55 year old stand of European oak (*Quercus robur*) and a minor fraction of silver birch (*Betula pendula*), with a younger understory of European beech (*Fagus sylvatica*). The oak stand extends to about 250 m to the west and 40 m to the east. The forest canopy at the west tower is 24–26 m high and had a leaf area index (LAI) of 3.0 in July 2003. The main tower is located within an area dominated by beeches and birches. West of the main tower (main wind direction) is a stand of 65 year old beeches (90%) and birches (10%), an older forest of similar composition as that in the east, and an oak forest (*Q. robur and Q. rubra*) about 50 m away in a south-western direction. The forest canopy west and east of the tower is 30 m high and exhibits a LAI of 3.5.

At both sites, sonic anemometers measured on the uppermost tower platform and the PTR-MS instruments were installed in containers at the base. The PTR-MS systems sampled air through $\frac{1}{4}$ inch Teflon (PFA=Perfluoroalkoxy) lines with an inner diameter of 3 mm. The details of the setup at both sites are described in Table 1. Data acquisition for the PTR-MS systems and the sonic anemometers was performed on different computers making a temporal adjustment of the time series necessary.

2.2 VOC measurements

Proton-Transfer-Reaction Mass Spectrometry (PTR-MS) utilises the ionisation of air constituents by reaction with

Table 1. Details of experimental setup at both towers.

	Main tower	West tower
Line and fitting material	PFA	PFA
Length of inlet line	50 m	60 m
Inner diameter	3 mm	3 mm
Flow rate	6 Sl min^{-1}	4–5 Sl min^{-1}
Height above ground / canopy	37/7 m	30/6 m
Distance of inlet to wind sensor	30 cm	20 cm
Line heating	none	5°C above ambient
Wind measurements		
Sonic anemometer type	USAT (METEK GmbH)	HS (GILL Instruments Ltd.)
Time resolution	10 Hz	5 Hz
PTR-MS instruments		
Total residence time of sample gas in drift tube+inlet system	∼1 s	<200 ms
Drift tube pressure	2.5 mbar	2.1 mbar
Drift voltage	400 V	580 V
E/N (E=electric field strength,	70 Townsend (Td)	130 Td
N=buffer gas density)	(1 Td=1×10^7 V cm^{-2})	

hydronium ions (H_3O^+) in a drift tube and subsequent detection of the protonated compounds by a mass selective quadrupole detector. Among the VOCs detectable by PTR-MS are many of the relevant biogenic compounds like isoprene and some of its oxidation products, monoterpenes, and methanol. Further details of this analytical technique may be found in literature (de Gouw et al., 2000; Lindinger et al., 1998). Here the focus is on the specific configuration of the two instruments deployed during the ECHO campaign. The instrument installed at the west tower was the commercially available PTR-MS manufactured by Ionicon with an optimised inlet system for fast time response (all tubing made of silcosteel with inner diameters of 0.5 and 0.25 mm). The PTR-MS operated at the main tower had a larger drift tube but had identical properties in all other relevant aspects. The configuration and characteristics of the two instruments are also included in Table 1.

2.2.1 Calibration

The two PTR-MS systems were calibrated against the same gas standards and were also compared against other measurement systems of various techniques in an extensive intercalibration experiment prior to the field campaign. Calibration gases were generated by capillary diffusion sources (Komenda et al., 2003; Schuh et al., 1997) and by dynamic dilution of custom prepared standard gases (Apel-Riemer Environmental Inc., Denver, CO). The gas standards contained methanol, acetaldehyde, acetone, isoprene, methyl vinyl ketone (MVK), and α-pinene at concentrations between 100 and 3000 ppbv. With help of a dynamic gas dilution system (Bronkhorst, NL), VOC concentrations between 100 pptv and 10 ppbv were produced. Zero air was generated

by directing humidified air (dew points of 5°–20°C) through a heated Platinum catalytic converter, which efficiently oxidised all the VOCs of interest present in air. All tubing and fittings of the gas dilution system were made of PFA Teflon.

For several ion masses, considerable offset signals are detected in the PTR-MS (Ammann et al., in 2004). Of particular importance in this context is the signal on mass 33 originating from oxygen isotopes ($^{16}O^{17}O^+$) or other potential interfering ions, which is in the same order of magnitude as the mass 33-signal (CH_3OHH^+) of typical methanol concentrations in ambient air. For the other four masses treated in this paper (M69, M71, M81 and M137), instrumental background counts were lower by at least one order of magnitude.
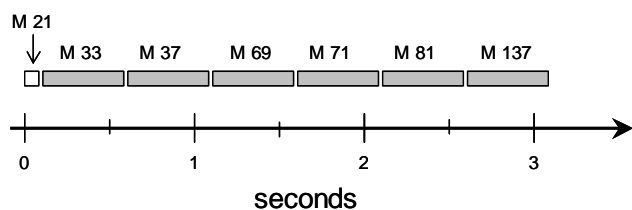
The attribution of ion masses to VOC compounds is a crucial problem of the PTR-MS method. Different ionised compounds with the same mass cannot be distinguished. Among BVOCs, this limitation concerns, for example, the oxidation products of isoprene, MVK and methacrolein (MACR), that are both detected at mass 71, or the various monoterpenes (α-pinene, β-pinene, limonene, sabinene, $Δ^3$-carene, etc.), all of them having a protonated ion mass of 137 amu. For these compounds, the measurement results are interpreted as a sum concentration of the respective components. Intercalibration and comparison with continuous GC-FID measurements during the ECHO project showed good agreement and demonstrated that the masses discussed in this paper (M33, M69, M71, and M137) can be allocated to the chemical species listed in Table 2 (Ammann et al., 2004).

2.2.2 Sensitivity and time resolution

The sensitivity of the PTR-MS for a certain VOC is determined by the kinetics of the proton transfer reaction, and

Table 2. Calibration factors for the compounds of interest in this study. *ncps=counts per second normalised to 1 million counts of primary ions.

Compound	Product ion mass [amu]	Calibration factor west tower instrument [ncps*/(μgm^{-3})]	Calibration factor main tower instrument [ncps*/(μgm^{-3})]
Methanol	33	10.8	5.4
Isoprene	69	6.4	4.9
Sum monoterpenes	137	1.4	0.9
MVK+MACR	71	13.1	10.3

Fig. 2. Typical measurement cycle, with dwell times of 0.1 s for primary ions and 0.5 s for other masses.

the instrument and mass specific detection efficiency (transmission). Some product ions undergo collision-induced fragmentation, depending on the operating pressure and electric field in the drift tube. Among the VOC species investigated here, protonated isoprene and monoterpenes can fragment significantly. As only part of the resulting products can unambiguously be detected, fragmentation has to be accounted for in the calibration. The fragmentation patterns can reasonably be assumed constant as long as the operation parameters of the PTR-MS are not changed. The calibration is summarised in Table 2, showing the compounds of interest for this study with the corresponding masses and calibration factors. The differences in the sensitivities of the two instruments are mainly a result of different choices of kinetic energies in the two instruments.

The time resolution of the VOC measurements is of particular interest with respect to the use with the EC technique. The time response of PTR-MS measurements is limited by the integration time necessary to obtain sufficient counts of the respective ion mass and by the residence time of the analyte in the instrument. The signal of primary ions (detected as $H_3^{18}O^+$ on mass 21) was $6 \times 10^3 - 1 \times 10^4$ counts per second (cps) corresponding to a $H_3^{16}O^+$-signal of $3 - 5 \times 10^6$ cps. The signals of the masses related to VOCs were in the order of 10^2 cps/ppbv. For typical ambient concentrations of one ppbv or less, an integration time of 0.2–0.5 s is necessary to avoid important noise contributions due to counting statistics. The maximum time response for the measurement of a single compound is therefore in the order of 5 Hz. As the quadrupole detector only allows subsequent detection of dif-

ferent ion masses, the achievable time resolution decreases with the number of scanned masses. When measuring several masses, the number of masses determines the time resolution, and not the residence time of the analyte in the PTR-MS, even in the case of the instrument with the larger drift tube (Table 1). During ECHO, six to eight different masses were measured, resulting in typical measurement cycles of 3 seconds length as illustrated in Fig. 2.

2.2.3　Effects of inlet lines

Besides the instrumental characteristics described above, the time resolution of the VOC measurements is also affected by the sampling configuration with 50–60 m long inlet lines. Fast concentration changes are attenuated as a consequence of differential flow speed across the tube diameter and small scale turbulence within the tubes. This high frequency damping sampling through long tubes can be described by spectral transfer functions, which specify the attenuation in dependence of the frequencies (Lenschow and Raupach, 1991). Karl et al. (2002) confirmed experimentally that these spectral transfer functions produce realistic estimates for the damping of VOCs aspirated through PFA Teflon tubes. In the configuration of this study (60 m long PFA tube with an inner diameter of 3 mm, and a typical flow of 5–6 litres min^{-1}, Reynolds numbers of $\sim$2300–2700), the transfer functions predict a relevant damping only for frequencies above 1.5 Hz, even if unfavourable laminar flow conditions are considered.

Another potential problem of long inlet lines are chromatographic effects for compounds having a high affinity to the tube surfaces. For clarification, experiments with standard gases were performed at both tower sites. A Tedlar bag containing a mixture of methanol, isoprene and α-pinene in nitrogen was connected to the inlet on top of the tower via a three-way Teflon (PFA) valve. In the default position (0) of the valve, the flow corresponded to the regular setup; air flowing from the inlet next to the sonic anemometer down to the PTR-MS. The other position (1) connected the sampling line with the Tedlar bag. By manually switching the valve from position 0 to 1 and back, pulses of high VOC concentrations were sent through the inlet line. The PTR-MS at the base of the tower was operated in a mode
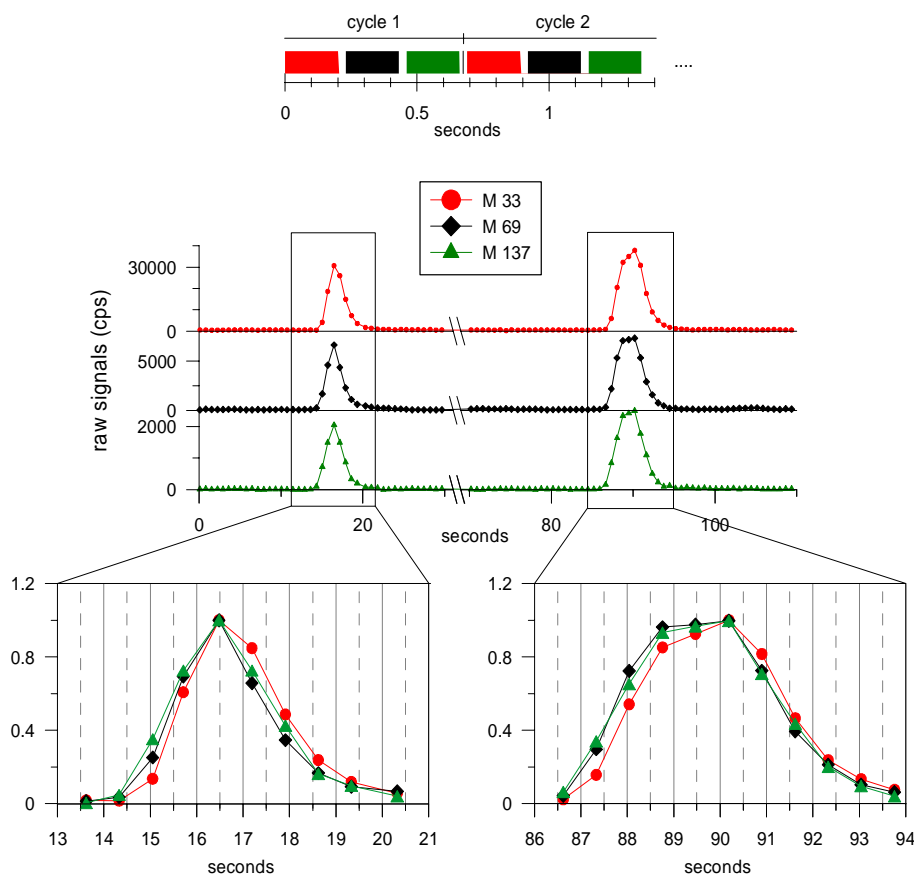
Fig. 3. Measurements of two concentration pulses as generated by aspirating a standard gas through the 60 m long inlet lines. Top: visualisation of the sequential measurement of the three masses within one measurement cycle, middle: raw signals of the PTR-MS, and bottom: peaks normalised to maximum concentration.

measuring the corresponding masses in a measurement cycle of 1 s or less. Figure 3 shows the measurements of two concentration pulses generated by such an injection of calibration gas at the top of the tower. The upper diagram displays the PTR-MS raw signals (counts per second) of the respective masses (M33 representing methanol, M69 isoprene, and M137 monoterpenes), whereas the bottom diagram shows a magnified display of the two pulses, in which the signals are normalised to the maximum of the peak.

Within the time resolution of the PTR-MS, no significant delay from one peak to another was observed. In fact, the slight deviations of the single normalised peaks are consistent with the time difference between the actual measurements of the single masses within one measurement cycle. As illustrated in the top part of Fig. 3, the three masses were successively integrated for 0.2 s. However, the data are logged on a cycle basis, meaning that the recorded measurement times for the three masses of one particular cycle are identical, although in reality they are shifted by 0.2 s (plus a small delay time necessary to adjust the quadrupole mass filter from one mass to the next). These delays correspond almost exactly to the lag of the different mass peaks. It demonstrates that there were no significant differences in the attenuation of one VOC relative to another in the inlet tube, at least not within the chosen time resolution of the flux measurements (0.5–0.25 Hz). Besides the compounds/masses presented in Fig. 3, acetaldehyde, methyl ethyl ketone, and toluene were investigated in the same manner and the results were identical. To quantitatively check for losses, a second inlet line experiment was carried out. Instead of manually generating pulses of VOC concentrations, a cylinder with standard gas and a mass flow controller (MFC) was used to generate better defined pulses of concentrations. The standard gas was added to zero-air for about 5 s providing mixing ratios at the inlet of 5 to 20 ppb. Based on the precision of the MFC and the uncertainty related to the instantaneous opening/closing of the MFC, the accuracy of the summed concentration of such a pulse was estimated to be ±20%. The integral VOC concentrations as measured by the PTR-MS at the base of the tower were within this range for all compounds. The comparison of the results with a heated (5–10°C above ambient temperature) and non-heated inlet line showed no significant differences for any of the VOCs discussed here.
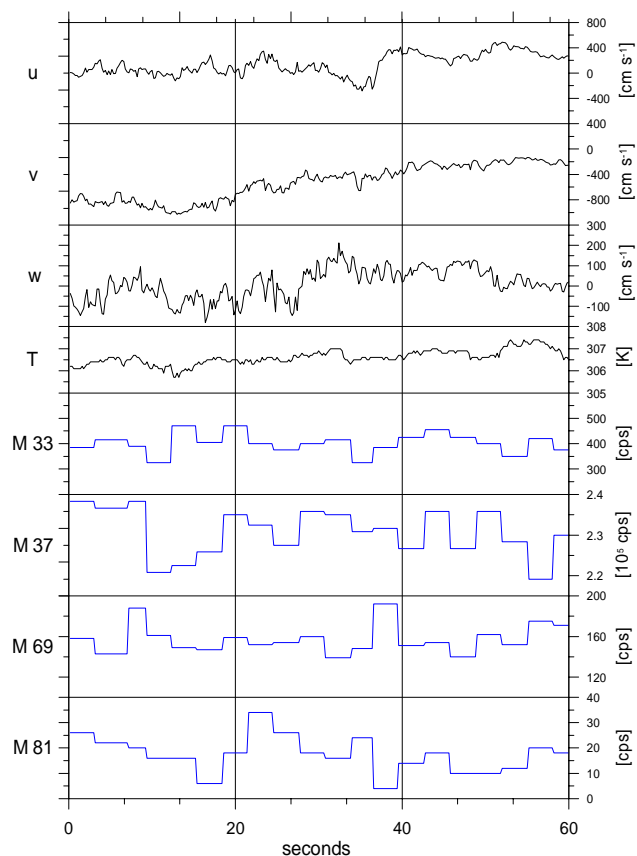
Fig. 4. Plot of sonic anemometer data (black) and PTR-MS data after expansion (blue).

2.3 Calculation of fluxes

2.3.1 Eddy Covariance

The EC flux of a scalar c is equal to the covariance of the vertical wind w and c. If w and c are continuously measured at a given point with a constant time step Δt, the scalar flux can be determined as:

$$F_c = \frac{1}{n} \sum_{i=1}^{n} (w_i - \bar{w}) \cdot (c_i - \bar{c}) \qquad (1)$$

w_i and c_i are the instantaneous values of vertical wind and scalar concentration, $\bar{w}$ and $\bar{c}$ are the means over the integration interval, and n corresponds to the number of equidistant individual measurements within the integration interval $T_a = n \cdot \Delta t$, usually between 10 and 60 min. The determination of a flux by Eq. (1) is valid if the turbulent elements (eddies) are advected past the measurement sensor in a stationary flow and the eddies are assumed to remain unchanged during this transport (Taylor hypothesis, see e.g. Stull, 1988).

If the scalar is measured by aspirating the sample gas through an inlet line, the corresponding fluctuations of the

scalar and the wind are time-displaced. The EC flux is then given by

$$F_c \left(\tau_{eff} \right) = \frac{1}{n} \sum_{i=1}^{n} (w_i - \bar{w}) \cdot \left(c_{i + \frac{\tau_{eff}}{\Delta t}} - \bar{c} \right), \qquad (2)$$

where τ_{eff} is the time lag between the two series $w(t)$ and $c(t)$. A spatial separation of the wind sensor and the scalar sampling point along the wind direction also contributes to the effective time lag.

The covariance between w and c as a function of the lag is called the covariance function $F_c(\tau)$. It is most efficiently calculated via transformation of the time series into the frequency domain by application of fast Fourier transformations, multiplication of the Fourier spectra and subsequent back-transformation. If there is a vertical flux, the covariance function exhibits a maximum at the effective lag between the measurements of w and c.

Wienhold et al. (1994) proposed to use the fluctuation of the covariance function at τ values far away from the true lag as an estimate for the precision of an individual flux determination. The idea of this error determination is that the signal of the flux at the true lag needs to exceed the general noise of the covariance function. We adopt this approach and determine the standard deviations of the covariance function in the ranges $\tau = -180$ s to -160 s and $\tau = 160$ s to 180 s. These delay times correspond to several times the integral timescale under turbulent conditions. It can thus be assumed that the vertical wind and the scalar are no longer correlated and the covariance function fluctuates around zero. The standard deviations at these lags characterise the noise of the covariance function. The averages of the threefold standard deviations in these ranges are used as a proxy of the precision and also characterise the detection limit of an individual flux measurement.

2.3.2 Eddy covariance for scalars with limited time resolution

The calculation of the EC flux in the frequency domain requires time series with the same time resolution for both wind and scalars. As described in Sect. 2.2.2, the time resolution of the VOC measurements was about 10 times lower than that of the wind and temperature records of the sonic anemometer. Based on theoretical turbulence spectra (Kaimal and Finnigan, 1994), it is assumed that the main portion of the flux is transported in eddies large enough to be resolved by the lower sampling frequency of the VOC measurements. Expecting only a minor loss by neglecting high-frequency concentration changes, an individual VOC measurement by the PTR-MS is regarded to be representative for the whole time period of the measuring cycle (~3 s). Technically, this is implemented by simply repeating the PTR-MS mass concentrations of a particular cycle (according to the time resolution of the wind measurements) until the next PTR-MS data point is available. Figure 4 illustrates the effect of this procedure

on the time series of the PTR-MS data. After this treatment, the VOC data are equidistant with the same time resolution like the wind time series, allowing a spectral analysis of the measurements. This brings the advantage of calculating the covariance function in the frequency domain and several established quality control procedures for EC data can be applied (Aubinet et al., 2000; Foken and Wichura, 1996). This convenience comes at the cost of losing flux contributions at high frequencies.

Another issue complicating the direct EC flux calculation is the time difference between the sonic anemometer and PTR-MS measurements. The long inlet tubes from the top of the towers to the PTR-MS installed on the ground lead to a general delay between the measured time series of the sonic anemometers (wind and temperature) and the mass concentrations of the PTR-MS. In addition, the data of the two instruments were collected on different computers. Although the internal clocks of these computers were synchronised about twice a day in reference to a radio clock, deviations in the order of seconds in either direction between the two systems occurred. For these reasons, the effective lag between the wind data and PTR-MS data is only known within a range of a few seconds.

Given these circumstances an algorithm for the EC flux calculation that does not depend on the knowledge of the lag was applied. In short, the procedure involved 5 steps.

1. Rotate the wind data to obtain zero vertical wind speeds and apply a linear de-trending to all time series for the integration period of 30 min.

2. Transform the time series into the frequency domain with a fast Fourier transformation.

3. Compute the cross-spectra of vertical wind and scalar quantities.

4. Calculate the covariance functions between w and scalars through back-transformation of the cross-spectra into the time domain.

5. Identify the effective lags τ_{eff} from the maxima of the covariance functions and set the fluxes equal to these covariances $F_c(\tau_{eff})$.

If no maximum can be identified in the expected lag window, an unambiguous determination of the flux is not possible. In these cases the confidence interval for the flux value around zero was estimated by the above defined method for determining the precision of an individual flux measurement. This quantity corresponds to the lag-independent noise in the covariance function.

Figure 5 shows an example of covariance functions from a multi-component flux measurement by PTR-MS. For comparability, the covariance functions $F_c(\tau)$ were divided by the standard deviations of w and c, yielding the corresponding
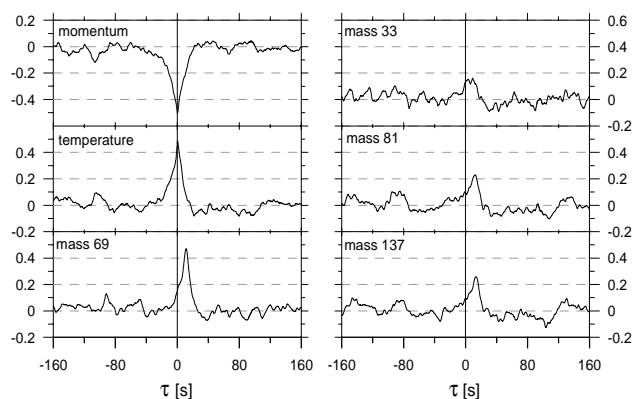

Fig. 5. Correlation functions for a flux calculation of an exemplary 30 min interval (15 July 2003 13:00–13:30).

correlation functions $r_{wc}(\tau)$. While the lag (location of maximum) is close to zero for temperature and momentum (measured by the sonic anemometer), significant positive lags are observed for the PTR-MS mass signals. Using the individually determined delays, cross-spectra were lag-corrected and co-spectra (real part of the cross-spectra) were calculated for the following spectral analysis procedures.

2.3.3 Quality control of fluxes

Beside the described evaluation of the covariance function, the ogive analysis (Oncley, 1989) is used for an effective quality control of the EC fluxes. The finite ogive $Og(f)$ is defined as the sum function of the co-spectrum (Co_{wc}), over the frequency range given by the sampling interval T_a and the time resolution. The lowest resolvable frequency (f_{low}) is determined by $(2 \cdot T_a)^{-1}$, the highest frequency (f_{high}) is $(2 \cdot \Delta t)^{-1}$ (Nyquist frequency).

$$Og_{wc}(f_m) = \sum_{i=0}^{m} Co_{wc}(f_m) \Delta f$$

$$m = 0, 1, 2, ..., \frac{N}{2} - 1, \ N = n \cdot \Delta t \qquad (3)$$

The ogive over all frequencies is equal to the covariance of the corresponding time series. Under ideal conditions and well-developed turbulence, the ogive starts at zero and monotonically approaches $F_c(\tau_{eff})$ with increasing frequency. Generally, flux contributions at the low and high end of the spectrum are small and the frequencies between 0.01 Hz and 0.1 Hz dominate, resulting in a typical S-shape of the ogive. Significant deviations from this form reflect disturbances of the eddy fluxes. If the ogive has a large slope at the lowest frequencies, significant fractions of the flux occur at these timescales, indicating that the integration interval may not be long enough to also capture these low frequent contributions. At certain frequencies, the ogives may exhibit turning points as a result of dominating fluxes in the opposite direction at
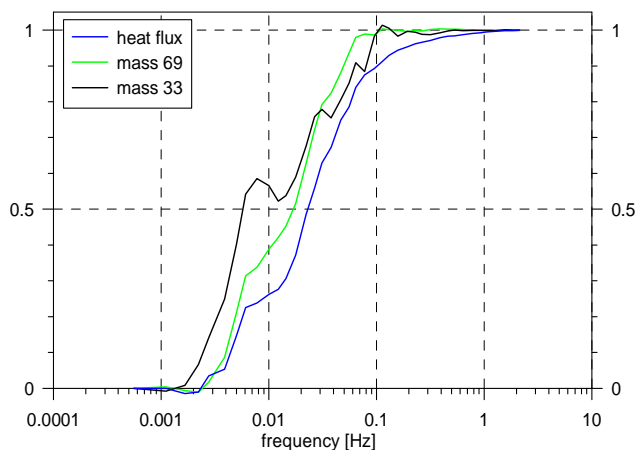
Fig. 6. Normalised ogives of heat, mass 69 and mass 33 fluxes on 18 July at 13:00.

those timescales. The occurrence of turning points indicates a violation of stationarity or homogeneity, and hence the basic assumptions for determining a flux by EC are questionable. As the raw co-spectra exhibit large scatter with increasing frequency, the resulting ogives also include considerable noise. For using the ogives as a quality criterion, a frequency smoothing is applied. The averaging interval is exponentially increased with increasing frequency, yielding a similar number of data points for each frequency decade (Kaimal and Finnigan, 1994). To compare the ogives of different scalars, it is convenient to look at normalised ogives (i.e. the ogives divided by the respective covariance flux).

Flux measurements are accepted if the normalised ogive has not more than one turning point and if its value at the frequency 0.002 Hz is smaller than 15%. Turning points are only accounted for in case the absolute difference from one point to the next exceeds 2% of the flux, thus a moderate noise level in the co-spectrum is tolerated.

The validity of a VOC flux measurement is assessed with two criteria. 1) The lag must be within a time window allowing plausible differences in the computer time and considering the residence time in the sampling tube, and the lags of different VOC masses must not differ more than the duration of a single PTR-MS measurement cycle. 2) The ogive of the heat or momentum flux, and the ogive of the VOC flux must meet the ogive criteria described above. Figure 6 shows an example of ogives from the west tower instrument on 18 July at 13:00. While the lag criterion applies to both isoprene and methanol, the flux of methanol is not acceptable, because the ogive exhibits too many frequency intervals with fluxes of opposite signs.

2.3.4 Compensation of high frequency losses

The sonic anemometer measuring the vertical wind speed as well as the temperature was operated at a time resolution of

5 Hz (west tower instrument). The heat flux and the momentum flux therefore encompass the frequency range from f_{low}=5.5×10⁻⁴ Hz (corresponding to an integration time of 30 minutes) to f_{high}=2.5 Hz (Nyquist frequency). The PTR-MS time series has artificially been brought to 5 Hz, but effectively has a lower time resolution. Flux contributions at the highest frequencies of the PTR-MS data are therefore lost, which is reflected in the ogives reaching their maxima at frequencies lower than f_{high}. The underestimate of the flux through the lack of high frequencies is determined by comparing the normalised ogives of the sensible heat and the VOC fluxes. It can be assumed that the frequency behaviour of temperature and VOCs are the same (Anderson et al., 1986; Moore, 1986) meaning their normalised ogives are identical. In the case of high-frequency damped VOC fluxes, the ratio of the normalised ogives $\frac{Og_{wT}(f)}{Og_{wVOC}(f)}$ is smaller than one below the cut-off frequency and its difference to one corresponds to the fraction of the flux lost due to the damping. Therefore, the VOC fluxes reported here were corrected by the mean of these differences at f=0.1 Hz and f=0.067 Hz.

The performance of this correction and potential effects from the expanding of the PTR-MS data was examined with the 5 Hz temperature data of the west tower. Temperature time series of the same structure as the expanded PTR-MS data were generated by taking the temperature readings at the start of each PTR-MS measurement cycle and repeating it for the duration of this cycle. For an exemplary day, the heat fluxes from both this lower-frequency data set and the original 5 Hz data were calculated. The fluxes of the low-frequency data were on average 10.7% lower in comparison to the fluxes calculated from the original time series. The decrease represents the part of the flux that is lost by using the lower frequency data. After applying the correction described above, the covariance calculated from the low frequency data set falls well within the error range of the flux derived from the 5 Hz data. It should also be noted that the co-spectra derived from the expanded time series showed no additional signals in the frequencies related to the data expansion (∼0.3 Hz), as long as a flux was detectable from a clear maximum in the covariance function. In case of very small fluxes with unclear maxima, a spectral signal in the range of 0.2–0.5 Hz appeared.

2.4 Footprint calculations

The footprint of a flux measurement can be understood as a probability density function that describes how strongly a surface exchange at any location upwind of the sensor affects the measured flux. In order to calculate footprints for flux measurements in this study the analytical footprint model developed by Kormann and Meixner (2001) was applied. It is able to describe two dimensional footprints for receptors within the surface layer under non-neutral conditions and is simple enough to be routinely applied for the analysis of flux measurements.
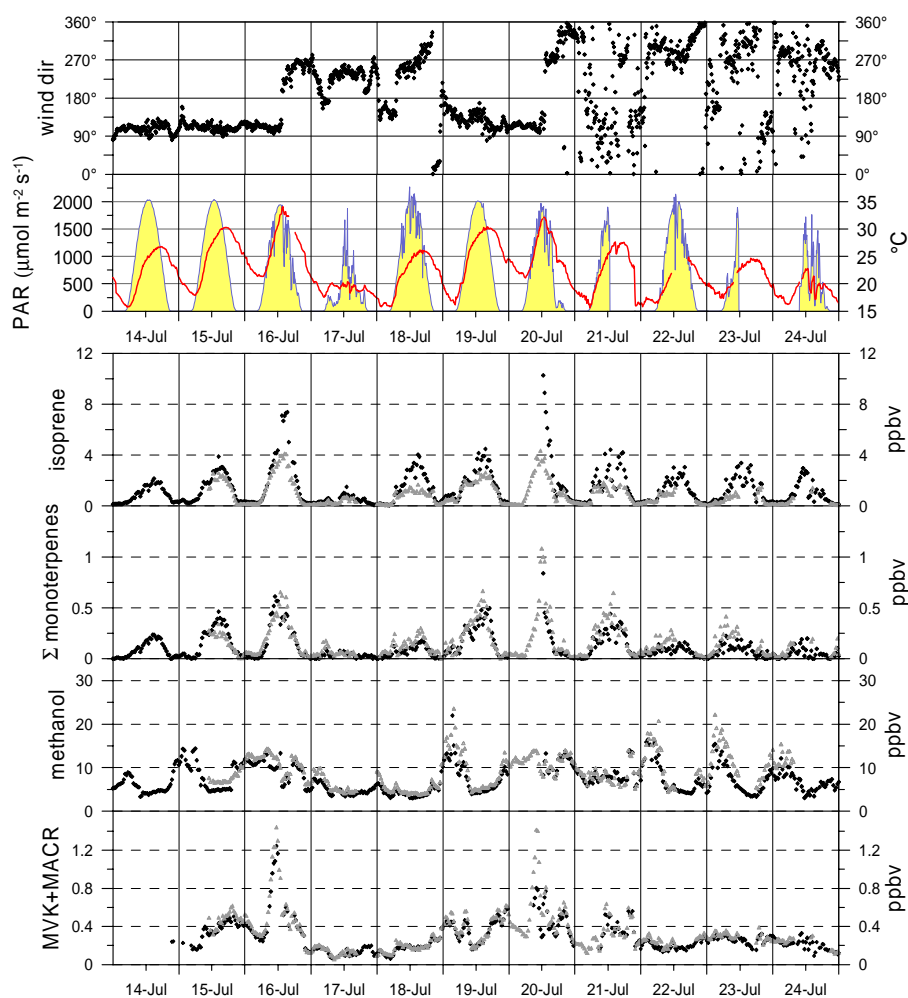
Fig. 7. VOC mixing ratios as determined from PTR-MS measurements, black diamonds=west tower, grey triangles=main tower.

The footprint estimates from the model were combined with information from vegetation maps in order to study the contributions of different forest areas to the measured flux. For doing this analysis operationally, a Visual Basic macro module that can be conveniently executed within a spreadsheet was developed. Besides the relevant meteorological parameters for footprint models (friction velocity, stability, wind direction, cross-wind fluctuations), the program uses the coordinates of a number (unlimited, in principle) of quadrangular areas around the sensor as inputs. It then calculates the footprint area and the relative contribution of each quadrangle to the footprint. For the discussion of the measurements during ECHO, 11 quadrangles were defined around the west tower, according to the areas with different tree species compositions. As an example, the white-framed quadrangle in Fig. 1 represents the oak dominated part of the forest surrounding the west tower.

3 Results

3.1 VOC concentrations

The two PTR-MS systems were operated at the main and west towers during most of July 2003, whereas the EC measurements focused on the period from 13 to 24 July. This period was mostly characterised by clear sky conditions and high temperatures. The weather of the first half was influenced by an extended high-pressure area over Central Europe. Synoptic winds blew from eastern and south-eastern directions. Temperatures peaked on 16 July and fell after the transition of a cold front on 17 July. Figure 7 gives an overview of meteorological conditions during this period and the concentrations of ion masses related to BVOCs.

The concentrations of isoprene and the sum of monoterpenes exhibited the same diurnal pattern at both towers. Isoprene levels at the west tower exceeded those of the main tower on some occasions, whereas monoterpene concentrations differed less between the two locations, with
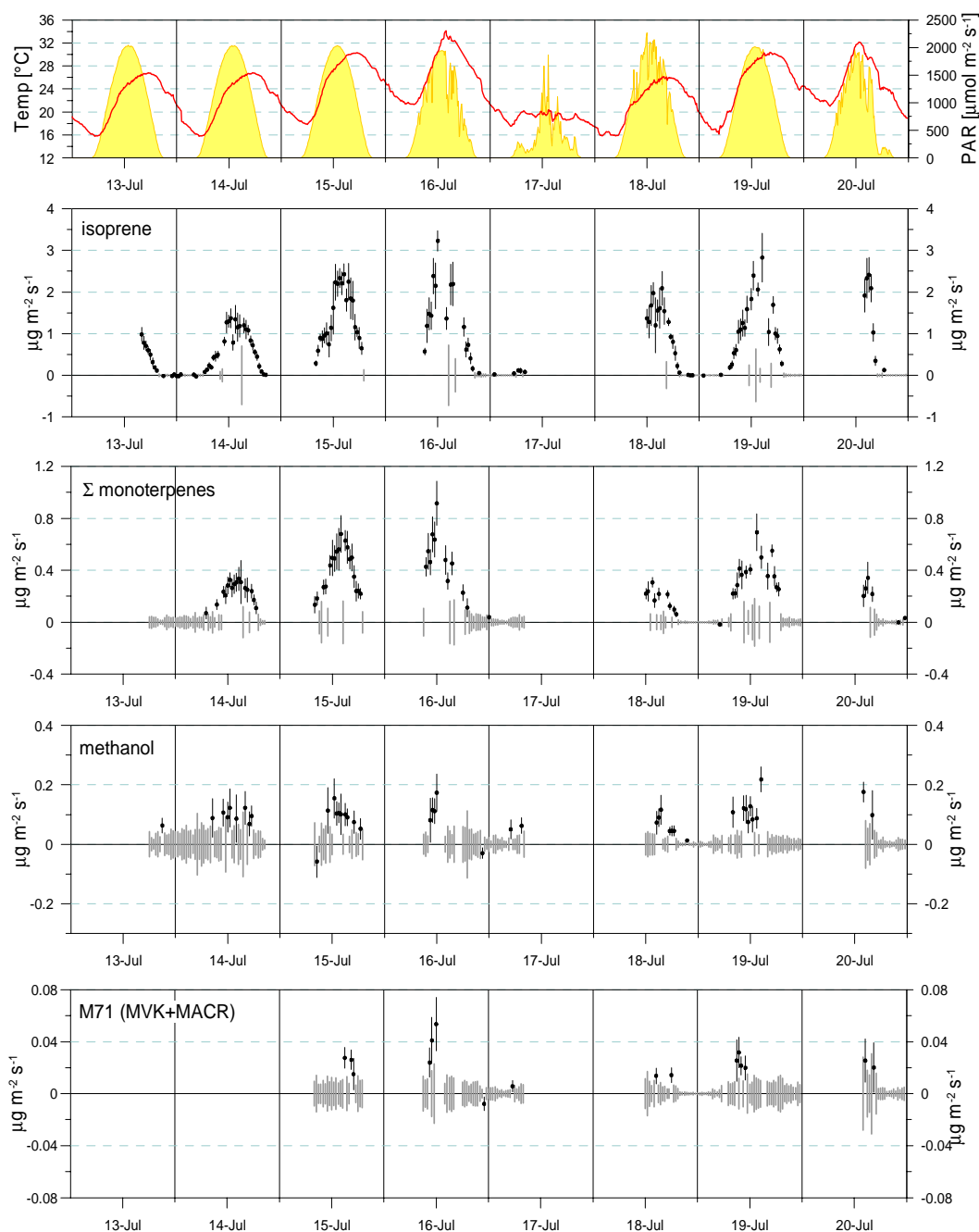
Fig. 8a. Fluxes of BVOCs at the west tower. Black error bars are the precisions of individual flux measurements, grey error bars denote the confidence interval in the cases where no fluxes could be determined.

more frequent observations of higher values at the main tower.

Among the compounds investigated, methanol (mass 33) generally exhibited the highest concentrations, behaving differently from isoprene and monoterpenes, with maximum values at night time and no clear repetitive diurnal variation. Often the highest levels of methanol occurred coincidently with high concentrations of toluene (data not shown), indicating an anthropogenic origin of these night time events.

Concentrations of mass 71, relating to the sum of the isoprene oxidation products MVK and MACR, were nearly identical at both sites. In contrast to their precursor, they often reached their maximum concentration later in the day, with exceptions on 16 and 20 July, when they peaked in the afternoon, with the decrease apparently related to the distinct shift of the wind direction on these days.
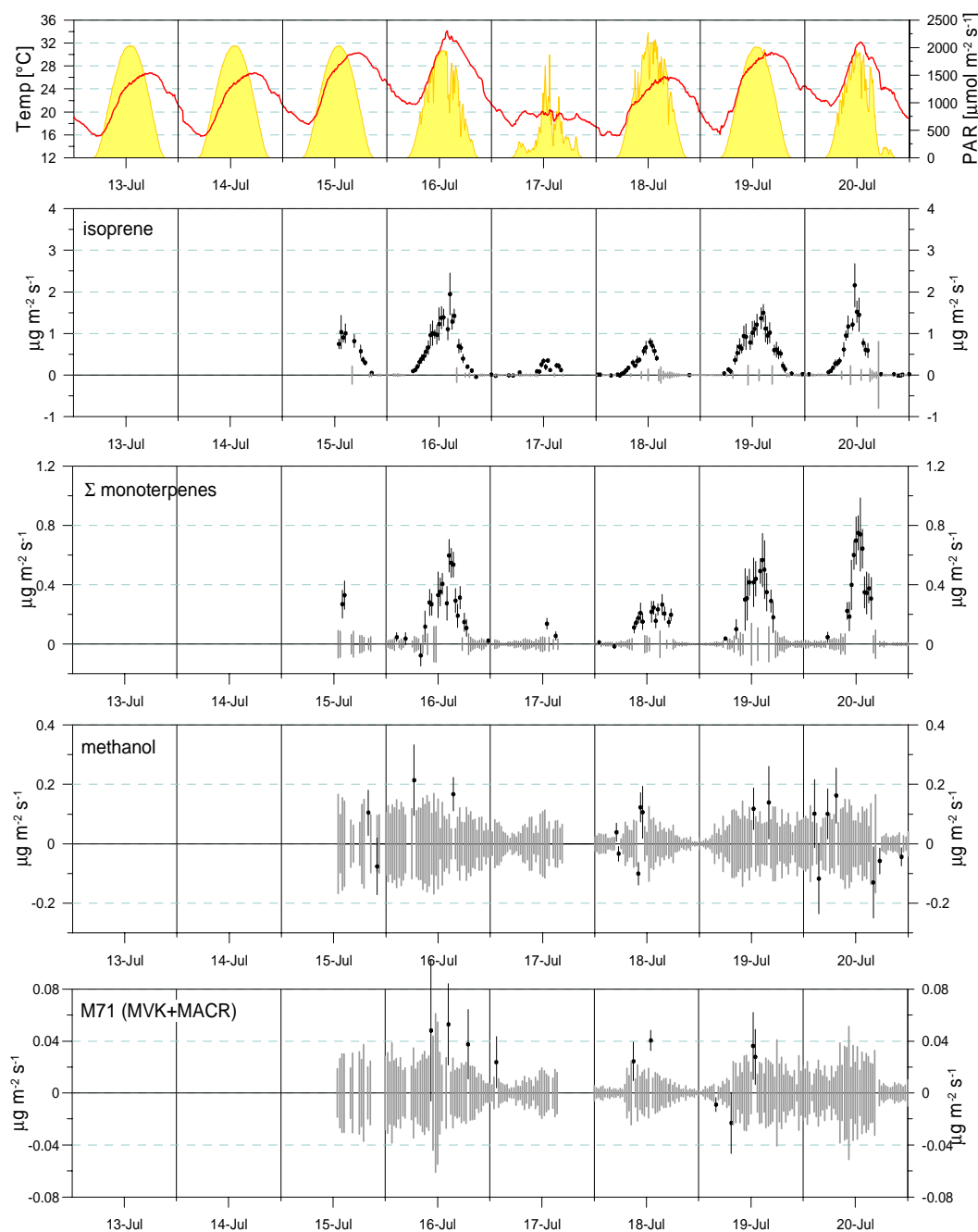
Fig. 8b. Fluxes of BVOCs at the main tower.

3.2 VOC fluxes

Between 13 July and 25 July both PTR-MS systems measured fluxes for a total of 366 (main tower) and 255 (west tower) half hour periods. During most of this period, isoprene, its oxidation products MVK+MACR, methanol, and the sum of monoterpenes were measured simultaneously. The time series of fluxes at the two towers that passed the quality criteria are presented in Figs. 8a and b. Gaps in these time series represent periods when the PTR-MS systems were not operated in EC mode or were offline because of maintenance (e.g. west tower instrument on 20 July). The error bars denote the precision of individual flux measurements representing three times the standard deviation of the corresponding covariance function at time shifts far away from the expected lag (as described in 2.3.1). Grey error bars (around zero) are plotted in the event of rejected fluxes. The data selection based on the quality criteria defined in 2.4
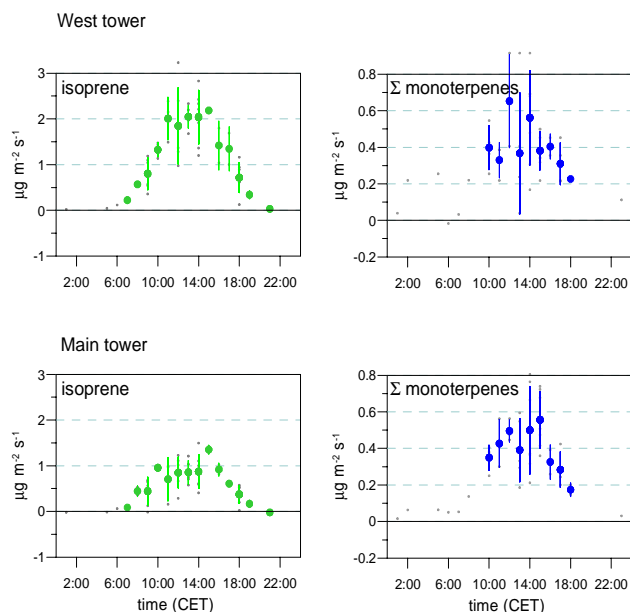
Fig. 9. Mean hourly fluxes of isoprene and monoterpenes during days with simultaneous measurements at both towers. Small symbols are individual measurements, large circles are hourly means, and error bars are the corresponding standard deviations.

resulted in a rejection of 45% to more than 90% of the flux measurements, depending on the compound.

The high frequency damping factor as determined from the comparison of temperature and VOC ogives was in an acceptable range. In the case of the isoprene fluxes, the damping factor was on average 11% for the instrument on the west tower and 16% at the main tower. For the whole data set collected, the losses were fairly stable (1st and 3rd quartile were 7 and 15%, respectively), and did not depend on stability or wind speed. The damping factors for other VOCs did not differ significantly and also showed no dependence on stability or wind speed.

Highest emission fluxes were found for isoprene. The daytime fluxes of the sum of monoterpenes were also clearly above the detection limit of both flux measurement systems. The fluxes of methanol were significantly lower, only detectable during the day. MVK+MACR fluxes hardly exceeded the detection limit, and only an order of magnitude estimate of these fluxes could be derived from measurements in this study. No systematic deposition fluxes could be detected for either of the compounds investigated here.

In order to compare the results of the flux measurements at both towers, the mean daily fluxes of isoprene and the sum of monoterpenes during the days with simultaneous measurements at both sites were looked at, as shown in Fig. 9. Isoprene fluxes were higher at the west tower (1.25 versus $0.61\,\mu\mathrm{g\,m}^{-2}\,\mathrm{s}^{-1}$, on average) and the fluxes of monoterpenes were comparable at both sites (0.33 at the west and $0.37\,\mu\mathrm{g\,m}^{-2}\,\mathrm{s}^{-1}$ at the main tower)

3.2.1 Standardisation of fluxes

Because many of the biogenic VOCs are emitted in dependence on temperature and light, it is useful to normalise the emissions to standard temperature and radiation conditions (usually 30°C and 1000 μmoles m^{-2} s^{-1} PAR). At the leaf level, isoprene emissions (E_{leaf}) are related to the standard emission (E_{std}) by

$$E_{leaf} = E_{std} \cdot C_L\,(PAR) \cdot C_T\,(T),\qquad(4)$$

where, $C_L(PAR)$ and $C_T(T)$ are dimensionless functions describing the light and temperature dependence (Guenther, 1997), referred to as G97 algorithm. For the purpose of using this model for standardising above canopy fluxes, the orientation of the leaves and shading effects within the canopy need to be considered. The total leaf area of a canopy is divided into a sunlit and shaded fraction, and the emission is described as

$$E_{canopy} = E_{std} \cdot C_T\,(T)$$
$$\cdot\left[LAI_{light} \cdot C_L\,(PAR_{light}) + LAI_{shade} \cdot C_L\,(PAR_{shade})\right],\quad(5)$$

where PAR_{light} and PAR_{shade} are the PAR experienced by the sunlit and shaded leaves, respectively, $LAI_{light/shade}$ are the leaf area indices of sunlit and shaded leaves in the canopy. The fraction of sunlit and shaded leafs as well as the corresponding PAR were estimated as a function of the solar elevation angle and measured PAR above the canopy, according to the canopy radiation transfer model described by Guenther et al. (1995). A single layer canopy was assumed, implying a homogeneous canopy with a spherical leaf angle distribution. Setting the observed emission flux equal to E_{canopy} in (5) yielded an average standard emission (E_{std}) of the leaves in this canopy. The resulting virtual standard emission factors for the west tower site were 0.8 μg m^{-2} s^{-1} for isoprene and 0.18 μg m^{-2} s^{-1} for the monoterpenes (average over the whole measurement period). On a ground area basis (LAI of 3, corresponding to LAI measurements at the west tower during July 2003), the standardised emissions of this canopy were 2.4 and 0.53 μg m^{-2} s^{-1} for isoprene and the sum of monoterpenes, respectively.

3.3 Footprint

The inhomogeneous species distribution within the forest around the two towers most likely caused major variations of the flux measurements. As a case study, the analytical model of Kormann and Meixner (2001) was used to estimate the footprints for the whole set of flux measurements at the west tower. Typical footprint extension along the wind direction was 200–300 m. Experimentally derived footprints from site specific wind tunnel studies were of the same magnitude (Aubrun et al., 2004), indicating that the model is able to predict realistic footprints despite its simple nature.

Considerable spatial inhomogeneities are expected for the emissions of isoprene, as this compound is mainly emitted by
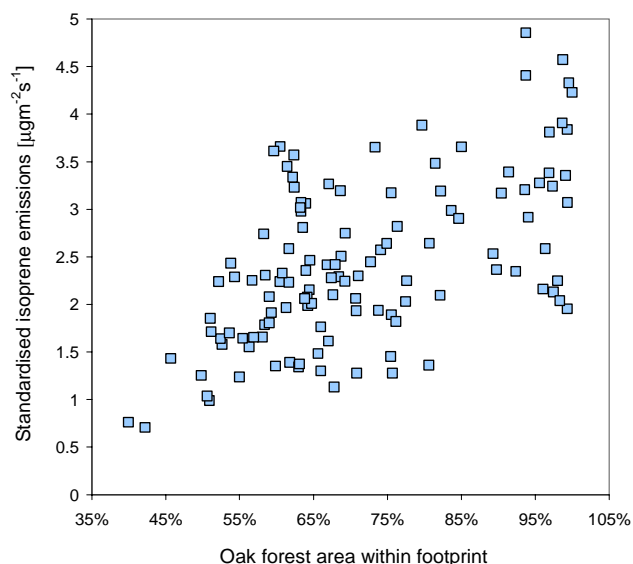
Fig. 10. Light and temperature normalised isoprene fluxes versus proportion of oak dominated forest within footprint areas.

Fig. 11. Comparison of fluxes calculated from expanded data (not corrected for high frequency losses) and from disjunct VOC time series.

oaks, which cover only certain sections of the forest around the tower. The footprint model was used to determine the fractions of oak dominated forest within the footprints of single measurements. The measured isoprene flux was then correlated with this oak fraction. Since isoprene fluxes are expected to be mainly controlled by light and temperature in the short term, the measured fluxes were first normalised to standard environmental conditions for this consideration. The canopy emissions were standardised as described in 3.2.1 and then plotted against the oak fraction in the footprint (Fig. 10). Cases with PAR below 100 μmoles m^{-2} s^{-1} were excluded from this analysis, as well as events with a significant footprint contribution from non-forested areas. The relationship between isoprene emissions and the proportions of oaks in the footprint is apparent.

4 Discussion

4.1 Methodical aspects

The EC method applied here includes an expanding of the PTR-MS data and treating them like a time series of the same (equidistant) time resolution as the wind data. This procedure results in a loss of information in the frequency range above 0.17 Hz. The overall high frequency losses of the VOC flux measurements were determined and corrected for by comparison with the heat flux spectra from unaltered temperature data. The high frequency damping derived in this way includes not only the effect of the PTR-MS data expansion, but also the attenuation caused by the long inlet tubes, the effects of sensor separation and the exchange
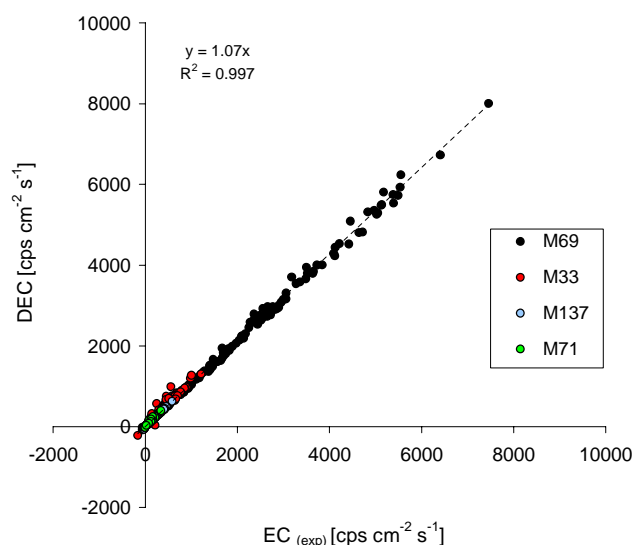
time of sample air in the PTR-MS drift tube. The resulting losses of the fluxes were fairly moderate, 11% and 16% for the west and main tower systems, respectively. These integral high-frequency losses were not significantly higher than the damping factor in the simulation with the temperature data (Sect. 2.3.4). It demonstrates that the data expansion is in fact dominating the high frequency damping and overlays all other effects. The difference in high frequency losses between the west tower and main tower system can be explained by the longer measurement cycle (3.5–4 s) at the main as compared to the west tower (3 s). The magnitude of these high frequency losses is in agreement with theoretical turbulence spectra (Kaimal et al., 1972). For an aerodynamic measurement height of 12 m (resulting from a geometrical height of 30 m above an estimated displacement height of 18 m=$\frac{3}{4}$ canopy height), Kaimal theory predicts a 11.5% and 15% flux contribution of frequencies above 0.1 and 0.16 Hz, respectively, under wind (3–4 ms^{-1}) and stability conditions ($-2<z/L<0$) as encountered during ECHO. The moderate high-frequency losses are therefore mainly a consequence of the dominating eddy timescales >3 seconds over a rough canopy such as the ECHO forest. The time resolution applied here would hardly be sufficient for flux measurements over areas with smaller roughness. The missing dependency of the high frequency damping on wind speed or stability is probably a consequence of the data selection, which resulted in a set of mainly daytime fluxes under similar conditions. As an additional check of the high frequency correction, the fluxes at the west tower were also calculated from the real 0.2 s data, by applying the virtual disjunct eddy correlation (DEC) technique (Karl et al., 2002). Figure 11 shows the uncorrected fluxes (in raw signals, i.e. cps cm^{-2} s^{-1}) from the

expanded data and the corresponding DEC data. The good correlation supports that the stability independent high frequency correction was appropriate. The slope of 1.07 shows that our high frequency correction of 11% resulted in 4% higher fluxes. While this difference is well within the measurement uncertainty, it indicates that even the DEC calculation suffers from high frequency losses, probably due to the combined effects of tube damping, sensor separation and mass integration time.

The goal of the measurements during ECHO was a characterisation of BVOC fluxes at this site, rather than a continuous VOC exchange measurement for the determination of a budget. Accordingly, the directive for quality control was not obtaining the best possible coverage of flux measurements, but ensuring a selection of trustworthy data. As can be seen in Figs. 8a and b, the resulting coverage of isoprene and monoterpene fluxes was still quite complete during daytime, whereas most of the methanol and MACR+MVK data were not suited for a flux determination. The large fraction of rejected data reflect the problematic nature of this site for performing flux measurements and the precision limits of the multi-component PTR-MS measurements. In most cases, the quality criteria of lag consistency (i.e. identifiable maximum in the covariance functions at realistic lags) and ogive shape responded redundantly. The main reason for rejections during night time were low wind speeds leading to a breakdown of turbulence, as documented by the ogives shapes of heat and momentum fluxes.

The detection limit derived from the fluctuations in the covariance function is not a constant value (Fig. 8). It depends not only on the correlating characteristics of the sonic anemometer and the PTR-MS instruments, but also on the instantaneous atmospheric conditions that are specific to each measuring site. The range of detection limits for different compounds does not directly correspond to the sensitivities of the PTR-MS (Table 2). For isoprene, monoterpenes and MVK+MACR, the observed detection limits are in line with the instrumental sensitivities, with highest sensitivity for the sum of MVK and MACR. However, the detection limits of methanol fluxes are not lower than those of isoprene and monoterpenes, despite the higher PTR-MS sensitivity for methanol. This is attributed to the higher ambient concentrations and background signals of mass 33 and their variability in comparison to other masses. Although most of the non-turbulent fluctuations will not appear in the covariance function as they are not correlated with vertical wind speed, they increase the general noise in the covariance function. Lowering the instrumental signal offset on mass 33 is one possibility to improve the performance of the measurement system for methanol fluxes.

4.2 Fluxes of biogenic VOCs

The fluxes of isoprene and monoterpenes exhibit strong diurnal patterns, consistent with light- and temperature-dependent emissions of these components from the forest. The tree species European oak (*Q. robur*), European beech (*F. sylvatica*) and silver birch (*B. pendula*) account for most of the biomass in this forest. Studies both in plant chambers and with branch cuvettes in the forest, confirmed light and temperature dependent emission of isoprene and monoterpenes (Dindorf et al., 2003).

In a radius of 100 m around the west tower, the leaf area contributions of beech, oak and birch were 48%, 44%, and 8%, respectively. Equation (5) relates the emissions of the forest canopy to an average standard emission factor at the leaf level. Assuming that isoprene is exclusively emitted from oaks at this site, this relationship was used to estimate the isoprene standard emission for oaks from the observed above canopy fluxes. The average standard isoprene emission (30°C, 1000 μmoles m^{-2} s^{-1} PAR at leaf level) of the canopy was 2.4 μg m^{-2} s^{-1} (ground area basis). Taking a typical dry weight of 320 g m^{-2} (Simpson et al., 1999) for oaks and using the oak fraction of 44%, this translated to a standard isoprene emission factor of 54 μgC g^{-1} h^{-1} (dry weight basis). The emission factor of *Q. robur* currently used in European emission inventories is 53 μgC g^{-1} h^{-1} (Simpson et al., 1999). This comparison confirms that the assumptions used in up-to-date VOC emission models are consistent with the magnitude of the measured isoprene fluxes.

Assuming that the remainder of the trees at this site were beeches (56%), and using the same dry weight per ground area, the basal emission rate of monoterpenes for beech (*Fagus sylvatica*) was estimated to be 9 μgC g^{-1} h^{-1}. Previous reports on the emissions of this species extend over a great range (Kesselmeier and Staudt, 1999; Schuh et al., 1997), the value derived here is in the upper range. Cuvette measurements on trees in the ECHO forest during 2002 and 2003 showed basal emission rates in agreement to our estimate, details of these results are presented elsewhere (Dindorf et al., 2005).

The small number of valid methanol fluxes does not allow a conclusion about the environmental control of methanol emissions. Only daytime upward fluxes could be observed on a regular basis, with an average of 0.087 μg m^{-2} s^{-1} (the average PAR and temperature of the same data set were 1315 μmoles m^{-2} s^{-1} and 26.3°C, respectively). This is in the range of recently reported methanol fluxes over a tropical forest (0.03–0.14 μg m^{-2} s^{-1} (Karl et al., 2004)), but lower than previous observations over conifer (Baker et al., 2001) and pine forests (Schade and Goldstein, 2001).

Based on the observations of high methanol concentrations on top of the tower and profile measurements throughout the canopy (Ammann et al., 2004), deposition of methanol is likely to occur, especially during night time. Assuming a methanol deposition velocity of 0.27 cm s^{-1} (Karl et al., 2004) and taking 10–15 ppb as the upper range of methanol concentrations observed above the canopy, deposition fluxes of 0.03–0.05 μg m^{-2} s^{-1} are plausible. Most of the time, this magnitude was below or close to the noise in

the covariance functions of mass 33 and vertical wind. The sensitivity of these systems was hence not sufficient to measure a systematic methanol deposition flux, albeit methanol deposition fluxes were observed in single cases. The rather momentary periods with high methanol concentrations indicate that strong methanol sources outside the forest may exist. Such strong emissions outside the typical fetch of our measurements can contribute to the observed irregularities in the ogives and may be one reason for the large number of non-acceptable methanol fluxes.

Fluxes of mass 71 (related to the isoprene oxidation products MACR and MVK) exceeded the detection limit of the flux measurement system only sporadically. The average upward flux during these (midday) events was 0.022 ($\pm$0,008) μg m^{-2} s^{-1}. Availing the picture of the forest as a chemical reactor, we can compare this flux with an estimated production of MVK and MACR from isoprene oxidation in the volume below the measurement sensor. With an observed mean OH concentration of 2.5×10^6 molecules cm^{-3} throughout the canopy (Hofzumahaus et al., 2003), 80 ppb of ozone, and 1.5 ppb isoprene (=mean mixing ratios during events with measurable fluxes of mass 71), the production of MVK and MACR from isoprene becomes 5.6×10^6 molecules cm^{-3} s^{-1} (rate constants and product yields according to the recommendations of IUPAC, http://www.iupac-kinetic.ch.cam.ac.uk). Considering this production as representative for the whole height below the EC measurement (30 m) and assuming that all products leave this virtual air column before being deposited or subject to further chemical transformation, a total MVK+MACR flux of 0.02 μg m^{-2} s^{-1} was derived. This estimate indicates that isoprene oxidation could in fact account for the magnitude of the observed mass 71 fluxes above the canopy. The data set gathered during ECHO is an ideal basis for a detailed investigation of the chemistry within the canopy and ongoing modelling activities may provide additional tests for this interpretation.

The presented results of the footprint calculations demonstrate that a rough classification of the fluxes according to the tree species composition of the source areas is possible. The scatter in the correlation (Fig. 10) is not surprising considering the uncertainties in the spatial vegetation classification as well as in the flux measurements, the normalisation with standard algorithms, and the footprint model. The general pattern in compatibility with the expected behaviour further supports the plausibility of the VOC flux measurements.

5 Conclusions

An eddy covariance method was successfully applied to determine BVOC fluxes at two measurement towers in the ECHO forest. A peculiarity of the applied EC calculation method is the technical increase of the VOC measurements' time resolution (originally 0.25–0.3 Hz) by repeating single measurements to obtain a time series equally spaced to the wind data (5–10 Hz). The inevitable high frequency loss through this procedure is accounted for by spectral analysis of the covariances of wind speed and scalars. A comparison with fluxes calculated from the real 0.2 s data by the DEC technique demonstrated that this high frequency correction was appropriate. Due to the dominance of eddy timescales below 0.5 Hz at this site, the resulting correction for the 0.3 Hz scalar measurements was only moderate. At this speed, the PTR-MS instrument can be used to measure the fluxes of several VOC compounds simultaneously. The presented method is able to handle non-exact time synchronisation of the instruments for wind and scalar measurements and significant high frequency damping effects. The tolerance in these respects enhances the practicability of this direct flux measurement method in field applications, where such limitations can be difficult to avoid.

Spectral analysis was used to discard measurements that violated the basic conditions for EC measurements. The generally large fraction of rejected flux data is a result of frequent breakdowns of turbulence during night time and reflects the complex nature of the measurement site with limited fetches in certain wind directions and pronounced inhomogeneities in the source area.

The validated fluxes of isoprene and monoterpenes are consistent with light- and temperature dependent emissions of these compounds by the dominating tree species (European oak, beech and birch) at this site. The above canopy fluxes were used for a top-down estimate of isoprene and monoterpene emission rates at the leaf level. The resulting basal emission rates (54 μgC g^{-1} h^{-1} isoprene from oak leaves and 9 μgC g^{-1} h^{-1} monoterpenes from beech) agree with results from cuvette measurements on trees in this forest. The plausibility of the flux measurements is further supported by the footprint analysis, which revealed that measured isoprene fluxes correlate with the abundance of oaks within the footprint.

Single events of upward MVK and MACR fluxes were also observed. The order of magnitude of these fluxes is compatible with an estimated production from isoprene oxidation throughout the forest canopy .

References

Ammann, C., Spirig, C., Neftel, A., Steinbacher, M., Komenda, M., and Schaub, A.: Application of PTR-MS for Measurements of Biogenic VOC in a Deciduous Forest, Int. J. Mass Spectrom., 239, 87–101, 2004.

Anderson, D. E., Verma, S. B., Clement, R. J., Baldocchi, D. D., and Matt, D. R.: Turbulence spectra of CO_2, water vapor, temperature and velocity over a deciduous forest, Agric. For. Meteorol., 38, 81–99, 1986.

Aubinet, M., Grelle, A., Ibrom, A., Rannik, U., Moncrieff, J., Foken, T., Kowalski, A. S., Martin, P. H., Berbigier, P., Bernhofer, C., Clement, R., Elbers, J., Granier, A., Grunwald, T., Morgenstern, K., Pilegaard, K., Rebmann, C., Snijders, W., Valentini, R., and Vesala, T.: Estimates of the annual net carbon and water exchange of forests: The EUROFLUX methodology, in Advances in Ecological Research, 30, 113–175, 2000.

Aubrun, S., Leitl, B., Schatzmann, M., and Koppmann, R.: Physical modelling of the vertical transport of biogenic emissions above a complex forest stand (ECHO site), Geophys. Res. Abstr., 6, 2004.

Baker, B., Guenther, A., Greenberg, J., and Fall, R.: Canopy level fluxes of 2-methyl-3-buten-2-ol, acetone, and methanol by a portable relaxed eddy accumulation system, Environ. Sci. Technol., 35, 1701–1708, 2001.

Baker, B., Guenther, A., Greenberg, J., Goldstein, A., and Fall, R.: Canopy level fluxes of measurements of 2-methyl-3-buten-2-ol by Relaxed eddy accumulation: field data and model comparison, J. Geophys. Res., 104, 26 104–26 114, 1999.

de Gouw, J. A., Howard, C. J., Custer, T. G., Baker, B. M., and Fall, R.: Proton-transfer chemical ionization mass spectrometry allows real-time analysis of volatile organic compounds released from cutting and drying of crops, Environ. Sci. Technol., 34, 2640–2648, 2000.

Dindorf, T., Kuhn, U., Dindorf, W., Ammann, C., Chaparro, G., Knothe, N., Steindel, F., Tritsch, C., Scheibe, M., Brancaleoni, E., Frattoni, M., Ciccioli, P., and Kesselmeier, J.: Effects of high ambient temperature on plant physiology and the emission of monoterpenes, isoprene, and volatile organic carbon by beech observed during ECHO-field campaigns in 2002 and 2003, EOS Trans. AGU, 84, Abstract A21A-04, 2003.

Dindorf, T., Kuhn, U., Ganzeveld, L., Schebeske, G., Ciccioli, P., Holzke, C., Köble, R., Seufert, G., Kesselmeier, J.: Emission of monoterpenes from European beech (Fagus sylvatica L.) as a function of light and temperature, Biogeosciences Discuss., 2, 137–182, 2005,
SRef-ID: 1810-6285/bgd/2005-2-137.

Foken, T. and Wichura, B.: Tools for quality assessment of surface-based flux measurements, Agric. For. Meteorol., 78, 83–105, 1996.

Guenther, A.: Seasonal and spatial variations in natural volatile organic compound emissions, Ecol. Appl., 7, 34–45, 1997.

Guenther, A.: The contribution of reactive carbon emissions from vegetation to the carbon balance of terrestrial ecosystems, Chemosphere, 49, 837–844, 2002.

Guenther, A., Hewitt, C., Erickson, D., Fall, R., Geron, C., Graedel, T., Harley, P., Klinger, L., Lerdau, M., McKay, W., Pierce, T., Scholes, B., Steinbrecher, R., Tallamraju, R., Taylor, J., and Zimmerman, P.: A global model of natural volatile organic compound emissions, J. Geophys. Res., 100, 8873–8892, 1995.

Guenther, A., Baugh, W., Davis, K., Hampton, G., Harley, P., Klinger, L., Zimmerman, P., Allwine, E., Dilts, S., Lamb, B., Westberg, H., Baldocchi, D., Geron, C., and Pierce, T.: Isoprene fluxes measured by enclosure, relaxed eddy accumulation, surface-layer gradient, mixed-layer gradient, and mass balance techniques, J. Geophys. Res., 101, 18 555–18 568, 1996.

Hofzumahaus, A., Siese, M., Rupp, L., Holland, F., and Schlosser, E.: HOx Radical Measurements During the ECHO Field Campaign in Summer 2003, EOS Trans. AGU, 84, Abstract A32A-0123, 2003.

Kaimal, J. and Finnigan, J.: Atmospheric boundary layer flows: Their structure and measurement, 289 pp., Oxford University Press, Oxford, 1994.

Kaimal, J. C., Wyngaard, J. C., Izumi, Y., and Coté, O. R.: Spectral characteristics of surface-layer turbulence, Q. J. R. Meteorol. Soc., 98, 563–589, 1972.

Karl, T., Guenther, A., Lindinger, C., Jordan, A., Fall, R., and Lindinger, W.: Eddy covariance measurements of oxygenated volatile organic compound fluxes from crop harvesting using a redesigned proton-transfer-reaction mass spectrometer, J. Geophys. Res., 106, 24 157–24 167, 2001.

Karl, T. G., Spirig, C., Rinne, J., Stroud, C., Prevost, P., Greenberg, J., Fall, R., and Guenther, A.: Virtual disjunct eddy covariance measurements of organic compound fluxes from a subalpine forest using proton transfer reaction mass spectrometry, Atmos. Chem. Phys., 2, 279–291, 2002,
SRef-ID: 1680-7324/acp/2002-2-279.

Karl, T., Potosnak, M., Guenther, A., Clark, D., Walker, J., Herrik, J. D., and Geron, C.: Exchange processes of volatile organic compounds above a tropical rain forest: Implications for modeling tropospheric chemistry above dense vegetation, J. Geophys. Res., 109, D18306, doi:10.1029/2004JD004738, 2004.

Kesselmeier, J., Ciccioli, P., Kuhn, U., Stefani, P., Biesenthal, T., Rottenberger, S., Wolf, A., Vitullo, M., Valentini, R., Nobre, A., Kabat, P., and Andreae, M. O.: Volatile organic compound emissions in relation to plant carbon fixation and the terrestrial carbon budget, Global Biochem. Cycles, 16, art. no. 1126, 2002.

Kesselmeier, J. and Staudt, M.: Biogenic volatile organic compounds (VOC): An overview on emission, physiology and ecology, J. Atmos. Chem., 33, 23–88, 1999.

Komenda, M., Schaub, A., and Koppmann, R.: Description and characterization of an on-line system for long- term measurements of isoprene, methyl vinyl ketone, and methacrolein in ambient air, J. Chromatogr. A, 995, 185–201, 2003.

Kormann, R. and Meixner, F. X.: An analytical footprint model for non-neutral stratification, Bound.-Layer Meteor., 99, 207–224, 2001.

Lamb, B., Westberg, H., and Allwine, G.: Biogenic hydrocarbon emissions from deciduous and coniferous trees in the United States, J. Geophys. Res., 90, 2380–2390, 1985.

Lenschow, D. H. and Raupach, M. R.: The Attenuation of Fluctuations in Scalar Concentrations through Sampling Tubes, J. Geophys. Res., 96, 15 259–15 268, 1991.

Lindinger, W., Hansel, A., and Jordan, A.: On-line monitoring of volatile organic compounds at pptv levels by means of Proton-Transfer-Reaction Mass Spectrometry (PTR-MS) Medical applicaitons, food control and environmental research, Int. Journal of Mass Spect. and Ion Processes, 173, 191–241, 1998.

Moore, C. J.: Frequency response correction for eddy correlation systems, Bound.-Layer Meteor., 37, 17–35, 1986.

Oncley, S. P.: Flux Parameterisation Techniques in the Atmospheric Surface Layer, PhD thesis, 202p., Univ. of California, Irvine, 1989.

Rinne, J. H. I., Guenther, A. B., Warneke, C., Gouw, J. A. D., and Luxembourg, S. L.: Disjunct eddy covariance technique for trace gas flux measurements, Geophys. Res. Lett., 28, 3139–3142, 2001.

Schade, G. W. and Goldstein, A. H.: Fluxes of oxygenated volatile organic compounds from a ponderosa pine plantation, J. Geophys. Res., 106, 3111–3123, 2001.

Schuh, G., Heiden, A. C., Hoffmann, T., Kahl, J., Rockel, P., Rudolph, J., and Wildt, J.: Emissions of volatile organic compounds from sunflower and beech: Dependence on temperature and light intensity, J. Atmos. Chem., 27, 291–318, 1997.

Simpson, D., Winiwarter, W., Börjesson, G., Cinderby, S., Ferreiro, A., Guenther, A., Hewitt, C. N., Janson, R., Khalil, M. A. K., Owen, S., Pierce, T. E., Puxbaum, H., Shearer, M., Skiba, U., Steinbrecher, R., Tarrason, L., and Öquist, M. G.: Inventorying emissions from nature in Europe, J. Geophys. Res., 104, 8113–8152, 1999.

Stull, R. B.: An Introduction to Boundary Layer Meteorology, 666 pp., Kluwer Academic Publishers, Dordrecht, 1988.

Wienhold, F. G., Frahm, H., and Harris, G. W.: Measurements of N_2O Fluxes from Fertilized Grassland Using a Fast-Response Tunable Diode-Laser Spectrometer, J. Geophys. Res., 99, 16 557–16 567, 1994.